Graphical Probabilistic Inference for Ground State and Near-Ground State Computing in QCA Circuits

(Accepted for Publication in IEEE Conference on Nanotechnology, 2005)

Sanjukta Bhanja* and Sudeep Sarkar†
* Electrical Engineering,† Computer Science and Engineering
University of South Florida, Tampa, Florida.
Emails: bhanja@eng.usf.edu, sarkar@cse.usf.edu

***Abstract*— We propose a graphical probabilistic Bayesian Network based modeling and inference scheme for Clocked Quantum-dot Cellar Automata (QCA) based circuit design that not only specify just the binary discrete states (0 or 1) of the individual cells, but also the probabilities of observing these states for *Ground (Most Likely) state computing*. The nodes of the Bayesian Network (BN) are the random variables, representing individual cells, and the links between them capture the dependencies among them. The modeling exploits the spatially local nature of the dependencies and the induced causality from the wave propagation and clocking schemes to arrive at a minimal, factored, representation of the overall joint probability of the cell states in terms of local conditional probabilities. This BN model allows us (1) to estimate the most likely (or ground) state configuration and the next lowest-energy configuration that results in output errors and (2) to show how weak spots in clocked QCA circuit designs can be found using these BN models by comparing the (most likely) ground state configuration with the next most likely energy state configuration that results in output error.**

***Index Terms*— QCA circuits, nanocomputing, energy minimization, computer vision**

I. Introduction

Quantum-dot Cellular Automata (QCA) is an emerging technology that offer a revolutionary approach to computing at nano-level [1], [2], [3]. It tries to exploit, rather than treat as nuisance properties, the inevitable nano-level issue of device to device interaction to perform computing. Other advantages include the lack of interconnects and electron transport. Research is ongoing for molecular-QCAs [4], which will make it possible to operate at room temperature, possibly alleviating the dominant criticism of this technology.

High level optimization of QCA circuit structure would require repeated estimates of ground (and preferably near-ground) states, along with cell polarizations, for different design variations. This is presently possible only through full quantum-mechanical simulation of the system evolution over time, which is known to be computationally expensive. The toolsets AQUINAS [5] and the Coherence vector simulation engine in the QCADesigner [6], both perform iterative quantum mechanical simulation (self consistent approximation, SCA) are very slow. In addition, they *cannot* estimate near-ground state configurations, which would be important for circuit error analysis. The toolsets such as QBert [7], Fountain-Excel simulation, nonlinear simulation [8], [6], and digital simulation [6] are fast iterative scheme, however, they just estimate the state of the cells and some fails to estimate the correct ground state for some situations. They do not estimate the cell polarization estimate. We present a modeling method that allows for not only cell polarization estimates for the ground state in a time-efficient manner, but also allows us to reason about other near-ground state configurations and hence generates the probability of the most probable erroneous states.

We propose the use of probabilistic models at layout level to model clocked QCA circuits. Given the strong *dependencies among devices* that need to be modeled, we use graphical probabilistic models, namely Bayesian networks, to explicitly represent dependencies and the inherent device-level uncertainties. In these representations, the nodes denote the random quantities of interest, which are the states of the QCA cells, and links denote direct dependencies, determined by causality induced by the direction of quantum signal propagation. The structure of the links are dictated by the layout of the devices and are quantified by conditional or joint probabilities, which are based on the quantum-mechanical density matrix. Probability computations is done by local message passing [9]. Using the Bayesian net model, we show not only how one can reason about *ground state configuration* but also the *lowest energy state configuration that results in output errors*.

II. Bayesian Model of Computation

We use the two-state approximate model of a single QCA cell following Tougaw and Lent [5] and other subsequent works on QCA. Each cell can be observed to be in one of two possible states, logical state 0, denoted by x_0, and the state 1, denoted by x_1. We will denote the probability of *observing* a QCA cell at state, x_i, by $P(X_i = x_i)$ or $P_{X_i}(x_i)$, or simply by $P(x_i)$[1]. The commonly used

[1]We will use upper-case to denote random variables and lower-case letters to denote values taken by the random variable.

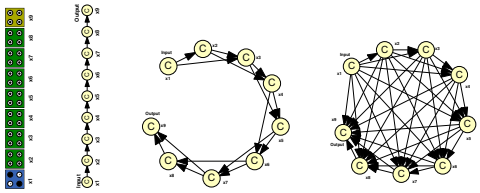

(a) (b) (c) (d)

Fig. 1. Bayesian net dependency model for (a) 9-cell QCA wire considering (b) 1-cell radius of influence (b) 2-cell radius of influence, and (c) all cells.

attribute of a *polarization* of a QCA cell can be expressed in terms of these state probabilities, $\delta_{X_i} = P_{X_i}(1) - P_{X_i}(0)$. The joint probability of observing a set of steady-state assignments for the cells is denoted by $P(x_1, \cdots, x_n)$. In terms of the underlying physics of the problem, this joint probability will be determined by the underlying quantum wave function over the possible states, which is quite large. To reduce the combinatorics, it is common to consider joint wave function in terms of product of wave function over one or two variables (Slater determinants), i.e. to consider a factored representation of the wave function (Hartree-Fock approximation).

Consider a linear arrangement of 9 QCA cells, shown in Fig. 1(a). Without making any assumptions, the joint state probability function can be decomposed into product of *conditional* probability functions by the repeated use of the property that $P(A,B) = P(A|B)P(B)$ (graphically shown in Fig. 1d).

$$P(x_1, \cdots, x_9) = P(x_9|x_8 \cdots x_1)P(x_8|x_7 \cdots x_1) \cdots P(x_2|x_1)P(x_1) \tag{1}$$

However, if one considers a 1 cell radius of influence, then a conditional probability $P(x_i|x_{i-1}, \cdots, x_1)$ can be approximated by $P(x_i|x_{i-1})$, and the overall joint probability can be factored as (graphically shown in Fig. 1b)

$$P(x_1, \cdots, x_9) = P(x_9|x_8)P(x_8|x_7) \cdots P(x_2|x_1)P(x_1) \tag{2}$$

If one were to assume a 2-cell radius of influence, then the factored joint probability will be,

$$P(x_1, \cdots, x_9) = P(x_9|x_8, x_7)P(x_8|x_7, x_6) \cdots P(x_2|x_1)P(x_1) \tag{3}$$

Bayesian Networks are graphical representation of the underlying dependency model. Note that directed link structure should not be interpreted as *the lack of dependence of a node on its children*, rather the direction just represents the cause-effect relationship. The dependence of node on its children is implicitly represented by the conditional probabilities.

A. Inferring and Quantifying Link Structure

The complexity of Bayesian network representation will be dependent on the order of the conditional probabilities, i.e. the maxium number of parents (N_p) a node. The maximum size of the conditional probability table stored will be 2^{N_p+1}. Note that since we use directional graph structure, we use the inherent causal ordering among the cells. Part of the ordering is imposed by the clocking zones. Cells in the previous clock zone are the drivers or the causes of the change in polarization of the current cell. Within each clocking zone, ordering is determined by the direction of propagation of the wave function [5].

Let $Ne(X)$ denote the set of all neighboring cells than can effect a cell, X. It consists of all cell within a pre-specified radius. Let $C(X)$ denote the clocking zone of cell X. We assume that we have phased clocking zones, as has been proposed for QCAs. Let $T(X)$ denote the time it take for the wave function to propagate from the nodes nearest to the previous clock zone or from the inputs, if X shares the clock with the inputs. Note that only the relative values of $T(X)$ are important to decide upon the causal ordering of the cells. We employ the breadth first search strategy, to decide upon this time ordering, $T(X)$.

The *causes*, and hence the parents $Pa(X)$, of X are the neighboring cells that are *either* in the previous clocking zone *or* nearer to the previous clocking zone *or* closer to the inputs than X. The children set, $Ch(X)$, of a node, X, will be the neighbor nodes that are not parents, i.e. $Ch(X) = Ne(X)/Pa(X)$.

The next important part of a Bayesian network specification involves the conditional probabilities $P(x|pa(X))$, where $pa(X)$ represents the values taken on by the parent set, $Pa(X)$. For arrangements of QCA cells, it is common to assume only Columbic interaction between cells and use the Hartree-Fock approximation to arrive at the matrix representation of the Hamiltonian given by [5]

$$\mathbf{H} = \begin{bmatrix} -\frac{1}{2}\sum_{i \in Ne(X)} E_k \delta_i f_i & -\gamma \\ -\gamma & \frac{1}{2}\sum_{i \in Ne(X)} E_k \delta_i f_i \end{bmatrix} \tag{4}$$

where the sums are over the cells in the local neighborhood, $Ne(X)$. E_k is the "kink energy" or the energy cost of two neighboring cells having opposite polarizations. f_i is the geometric factor capturing electrostatic fall off with distance between cells. δ_i is the polarization of the i-th neighboring cell. The tunneling energy between the two states of a cell, which is controlled by the clocking mechanism, is denoted by γ.

In the presence of inelastic dissipative heat bath coupling (open world), the system moves towards the ground state [5]. At thermal equilibrium, the steady-state density matrix is given by

$$\rho^{ss} = \frac{e^{-\mathbf{H}/kT}}{\mathrm{Tr}[e^{-\mathbf{H}/kT}]} \tag{5}$$

where k is the Boltzman constant and T is the temperature. Of particular interest are the diagonal entries of the density matrix, which expresses the probabilities of observing the cell in the two states. They are given by

$$\rho_{00}^{ss} = \tfrac{1}{2}\left(1 - \tfrac{E}{\Omega}\tanh(\Delta)\right),\ \rho_{11}^{ss} = \tfrac{1}{2}\left(1 + \tfrac{E}{\Omega}\tanh(\Delta)\right)$$

where $E = \frac{1}{2}\sum_{i \in Ne(X)} E_k \delta_i f_i$, the total kink energy at the cell, $\Omega = \sqrt{E^2 + \gamma^2}$, the energy term (also known as the Rabi frequency), and $\Delta = \frac{\Omega}{kT}$, is the thermal ratio. We are interested in these probabilities for the minimum energy ground state values. This is determined by the eigenvalues of the Hamiltonian (Eq. 4) which are $\pm\Omega$, a function of the kink energy with the neighbors. However, the states (or equivalently, polarization) of only the parents are specified in the conditional probability that we seek. The polarization of the children are unspecified. We choose the children states (or polarization) so as to maximize Ω, which would minimize the ground state energy over all possible ground states of the cell. Thus, the chosen children states are

$$ch^*(X) = \arg\max_{ch(X)} \Omega = \arg\max_{ch(X)} \sum_{i \in (Pa(X) \cup Ch(X))} E_k \delta_i f_i \quad (6)$$

The steady state density matrix diagonal entries with these children state assignments are used to decide upon the conditional probabilities in the Bayesian network (BN).

$$\begin{aligned} P(X=0|pa(X)) &= \rho_{00}^{ss}(pa(X), ch^*(X)) \\ P(X=1|pa(X)) &= \rho_{11}^{ss}(pa(X), ch^*(X)) \end{aligned} \quad (7)$$

III. Reasoning about QCA cells by Probabilistic Inference

Given the joint probability specification $P(X_1 = x_1, \cdots, X_n = x_n)$, as captured by the Bayesian network (BN) representation, we explore the computation of the following quantities of interest.

1) Given the polarization of the r input cells, $x_1, \cdots, x_r$, what is the *minimum energy* polarization (or most likely state) assignments of all the cells? For this we need to compute $\arg\max_{\{x_i\}} P(x_{r+1}, \cdots, x_N | x_1, \cdots, x_r)$, or the maximum likelihood state assignments. This can done using maximum likelihood propagation in the BN.
2) What is the minimum energy configuration that results in *error* at a output cell, x_s, for a given input assignment, $x_1, \cdots, x_r$? This can be arrived at, again, by conditional maximum likelihood propagation.

Using the above computations we can address QCA design issues such as, (i) What is a likelihood that a QCA circuit will result in correct output? (ii) What is lowest-energy state configurations that result in output errors. In the rest of this section, we outline the nature of the maximum likelihood propagation schemes that we will use to answer these questions.

The exact inference scheme is based on local message passing on a tree structure, whose nodes are subsets (cliques) of random variables in the original DAG [10]. This tree of cliques is obtained from the initial DAG

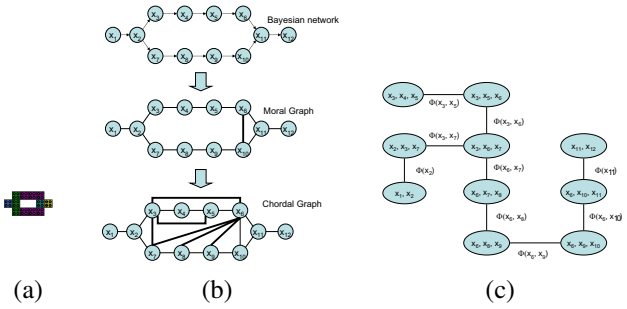

Fig. 2. (a) An arrangemnt of QCA cells (b) Transformation from a Bayesian network to a triangulated graph. (c) Junction tree of cliques.

structure via a series of transformations that preserve the represented dependencies and are necessary for the local message passing scheme. We illustrate this process using the simple arrangement of QCA cells in Fig. 2(a). First, we convert the DAG structure to a triangulated undirected graph structure via the construction of an undirected Markov structure, which is referred to as the *triangularized moral graph*, modeling the underlying joint probability distribution. An illustration of this process is shown in Fig. 2(b) (additional links added between parents and then further links are added for triangularization). In this triangulated graph, cliques C_i's are found. In practice, the triangulation and the clique enumeration steps is coupled [10]. We need to perform these transformations because it is proven [10] that these cliques can be arranged and connected as a junction tree 2c. Note that this structure is a special tree where there is unique path between any two cliques but if two (non-adjacent) cliques have a variable in common, this variable has to be present in all cliques that lie in the path connecting the two cliques. With each clique, C_i, in the junction tree we associate a function, $\phi(c_i)$, also termed as the probability potential function, over the variables in the clique, constructed out of conditional probabilities in the BN. For each conditional probability in the BN, $p(v|pa(X))$, we find one and only one clique, C_i, that contain the node set $\{V\} \cup Pa(X)$. The potential function for a clique is the product of the conditional probability functions mapped to that clique. Thus,

$$\phi(c_i) = \prod_{\{V\} \cup Pa(X) \in C_i} p(v|pa(X)) \quad (8)$$

The joint probability function, which was expressed as product of conditional probabilities, can now be expressed equivalently as product of the clique potentials.

$$p(x_1, \cdots, x_N) = \prod_v p(v|pa(X)) = \prod_{c_i \in C^t} \phi(c_i) \quad (9)$$

The tree structure is useful for local message passing. Given any observation (evidence), messages consist of the updated probabilities of the common variables between two neighboring cliques. Global consistency is automatically maintained by the junction tree [10].

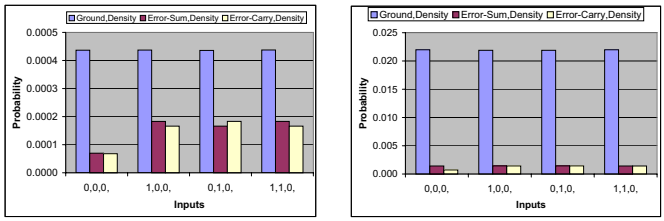

(a) (b)

Fig. 3. Probability of most likely state (ground) configuration that result in correct output and those minimum energy configurations that result in errors in the sum and carry output lines: (a) for the first design and (b) for the second design.

Maximum Likelihood Propagation: In the context of QCA circuits, it will be necessary to compute the ground state configuration and its probabilities. This can be cast as the maximum likelihood estimation problem. The ground state is given by the $\arg\max_{x_1,\cdots,x_n} p(x_1,\cdots,x_n)$. Since the problem of maximization of a product of probability functions can be factored as product of the maximization over each probability functions, this maximization can also be computed by local message passing [10]. The overall message passing scheme, the messages passed between two cliques using the maximum operator.

$\phi_i^*(s_{ij}) = \max_{\{C_i - S_{ij}\}} \phi(c_i)$; $\phi_j^*(s_{ij}) = \max_{\{C_j - S_{ij}\}} \phi(c_j)$

If message is being transmitted from C_i to C_j, then the scaling factor $\phi_i^*(s_{ij})$ is transmitted to clique C_j and probability distribution of C_j is rescaled where s_{ij} are common variables between C_i and and C_j.

Hence, $\phi(c_j) = \frac{\phi_i^*(s_{ij})}{\phi_j^*(s_{ij})}\phi(c_j)$

To find the configuration with this maximum likelihood probability, we start with the root clique, choose its most likely configurations. Then, we move on to its neighbors and choose their most likely configurations, constrained by the configuration of the separator nodes chosen in the root clique. The process continues to the neighbors of the neighbors and so on. The maximum likelihood probability can be computed by the product of the probabilities from the individual cliques.

Another analysis of interest when comparing QCA designs is the comparison of the least energy state configuration that results in correct output versus those that result in erroneous outputs. This is obtained by conditional maximum likelihood propagation where the next probable state probabilities are obtained.

Fig. 3 shows the probabilities of the most likely state (ground) configuration with correct outputs (shown in blue) and those minimum energy states configurations with error in the carry (shown in white) and sum output lines (shown in red), for four different inputs and for two design of full adders (shown in Fig. 3a and b). The second adder design is better than the first because the ratio of the probability of the erroneous state configuration to the probability of the correct configuration is lower than for the first design.

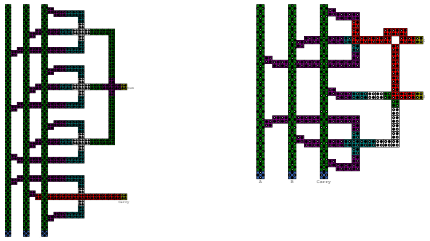

(a) (b)

Fig. 4. Differences in cell states (polarization), shown in red, between ground state and the energy state that results in erroneous outputs for an input vector of 1,0,0. The carry output most likely error modes for the *first design* are shown in (a) and the corresponding modes for the *second design* are shown in (b).

Apart from probabilities, we can also compute the most likely cell state configuration itself. For one input, Fig. 4 show the cells with erroneous states (shown as red cells) *between* least energy configurations resulting the correct output *and* the least energy configuration that results in error in the carry output lines. We found that, for different input combinations, the cell state errors in the first design start at the wiretaps, whereas the state errors in the second design start at the corners. These are weak spots in the respective designs that need to be reinforced.

We presented an efficient Bayesian network based probabilistic modeling for QCA circuit that can estimate ground state configurations, and near-ground state configurations for clocked designs, without the need for computationally expensive quantum-mechanical computations.

REFERENCES

[1] C. Lent and P. Tougaw, "A device architecture for computing with quantum dots," in *Proceeding of the IEEE*, vol. 85-4, pp. 541–557, April 1997.

[2] J. C. Lusth, C. B. Hanna, and J. C. Diaz-Velez, "Eliminating non-logical states from linear quantum-dot cellular automata," *Mirco-electronics Journal*, vol. 32, pp. 81–84, 2001.

[3] R. Kummamuru, J. Timler, G. Toth, C. Lent, R. Ramasubramaniam, A. Orlov, G. Bernstein, and G. Snider, "Power gain in a quantum-dot cellular automata latch," *Applied Physics Letters*, vol. 81, pp. 1332–1334, August 2002.

[4] C. Lent, B. Isaksen, and M. Lieberman, "Molecular quantum-dot cellular automata," *Journal of American Chemical Society*, vol. 125, pp. 1056–1063, 2003.

[5] P. D. Tougaw and C. S. Lent, "Dynamic behavior of quantum cellular automata," *Journal of Applied Physics*, vol. 80, pp. 4722–4736, Oct 1996.

[6] K. Walus, T. Dysart, G. Jullien, and R. Budiman, "QCADesigner: A rapid design and simulation tool for quantum-dot cellular automata," *IEEE Trans. on Nanotechnology*, vol. 3, no. 1, pp. 26–29, 2004.

[7] P. M. Niemier, M.T.; Kontz M.J.; Kogge, "A design of and design tools for a novel quantum dot based microprocessor," in *Design Automation Conference*, pp. 227–232, June 2000.

[8] G. Toth, *Correlation and Coherence in Quantum-dot Cellular Automata*. PhD thesis, University of Notre Dame, 2000.

[9] J. Pearl, *Probabilistic Reasoning in Intelligent Systems: Network of Plausible Inference*. Morgan Kaufmann Publishers, 1998.

[10] R. G. Cowell, A. P. David, S. L. Lauritzen, and D. J. Spiegelhalter, *Probabilistic Networks and Expert Systems*. New York: Springer-Verlag, 1999.